Clinical and Translational Oncology (2018) 20:1302–1313
https://doi.org/10.1007/s12094-018-1862-z

RESEARCH ARTICLE

Nur77 suppression facilitates androgen deprivation-induced cell invasion of prostate cancer cells mediated by TGF-β signaling

J. Wu[1] · H. Sun[2] · X. Yang[3] · X. Sun[1]

Received: 3 August 2017 / Accepted: 12 March 2018 / Published online: 28 March 2018

Abstract

Background Androgen deprivation therapy (ADT) remains a standard treatment for advanced prostate cancers. However, recent studies revealed that while inhibiting the growth of certain types of prostate cancer cells, ADT promotes invasion. In the current study, we explored the effects of Nur77, an orphan nuclear receptor, on prostate cancer cell invasion following ADT.

Methods Androgen receptor (AR) and Nur77 protein expression in patient tissues and cell lines were quantified via ELISA and western blot. The effects of AR-signaling on Nur77 expression were examined. The effects of Nur77 over-expression and knockdown on ADT-induced prostate cancer cell invasion were characterized.

Results The results showed that AR and Nur77 are both highly expressed in prostate cancers of patients. Nur77 is positively regulated by AR-signaling at transcriptional level in NCI-H660, a widely used prostate cancer cell line. AR antagonists, Casodex and MDV3100 treatment resulted in significant inhibition of prostate cancer cell growth but enhanced cancer cell invasion. Nur77 over-expression blocked invasion-promoting effect of ADT, which is consistent with the down-regulation of MMP9 and Snail protein expression. Further mechanistic investigations showed that Nur77 inhibited transcription of TGF-β target genes (Snail and MMP9), and thereby inhibits TGF-β-mediated prostate cancer cell invasion following androgen antagonism. In addition, our data suggested the nature of this inhibitory effect of Nur77 on TGF-β-signaling is selective, for Smad3-signaling, the classical effector of TGF-β-signaling, was not interrupted by Nur77 over-expression.

Conclusion Considering the limited success of management of prostate cancer metastasis following ADT, our data strongly suggest that Nur77 regulation could be a promising direction for search of complementary therapeutic strategy on top of classic ADT therapy.

Keywords Prostate cancer · Androgen receptor · Nur77 · Androgen deprivation · Cancer cell invasion

Introduction

Prostate cancer has long been one of the most common malignancies in men and a major cause of cancer death worldwide. Only in 2012, about 1.1 million new diagnoses and 307 thousand deaths of prostate cancer were reported [1]. Researchers have revealed that androgen and androgen receptor (AR) play pivotal roles during initiation and progression of prostate cancer. Activated by its native ligands, such as testosterone and 5α-dihydrotestosterone (DHT), AR and its downstream signaling pathways exert diversified functions under physiological conditions, and facilitate the initiation and progression of prostate cancer under pathophysiological conditions.

For patients with advanced or recurrent prostate cancer, androgen deprivation therapy (ADT) is now the standard

Electronic supplementary material The online version of this article (https://doi.org/10.1007/s12094-018-1862-z) contains supplementary material, which is available to authorized users.

✉ X. Sun
sunxzh1892@126.com

[1] Department of Urology, Drum Tower Hospital, Medical School of Nanjing University, 321 Zhongshan Rd, Nanjing 210008, Jiangsu, China

[2] Department of Urology, Nanjing First Hospital, Nanjing Medical University, Nanjing 210000, Jiangsu, China

[3] Institute of Business Analytics, University of Alabama, Tuscaloosa, AL 35401, USA

therapy [2]. As an anti-hormone therapy, ADT can down-regulate AR-controlled signaling to inhibit growth of prostate cancers [3]. However, the efficacy of ADT seems not to be sustainable, as prostate cancer cells will adapt to survive and grow [4]. In addition, recent studies showed that certain anti-androgen treatments increase invasion of cancer cells despite their inhibitory effects on growth of prostate cancer cells [5, 6].

Our research team has consistently studied on the roles of an orphan nuclear receptor, Nur77, in human cancers, especially the relationship between AR and Nur77 [7]. Nur77 (also known as TR3, NGFI-B or NR4A1) belongs to the NR4A family which consists of two other members, namely NR4A2 and NR4A3 [8]. Recent studies have demonstrated that Nur77 is implicated in numerous types of malignancies [9, 10]. Nur77 could induce apoptosis by direct interaction with Bcl-2 in the mitochondria, exposing proapoptotic BH3, or indirectly by stimulating other cytosolic proapoptotic proteins, such as BAX binding to the mitochondria to initiate the apoptotic cascade in cancer cells [11–13]. On the other hand, as a protein with diversified functions, Nur77 has also been reported to be a survival molecule which inhibits cancer cell death [14]. In prostate cancers, Nur77 has been shown to mediate IGFBP-3-induced apoptosis of 22RV1 prostate cancer cells [15, 16]. In addition, a recent study has shown that knockdown of Nur77 decreased anisomycin-induced cleavage of caspase-3, caspase-7 and PARP in prostatic cancer cells, indicating a stimulatory role for Nur77 in anisomycin-induced cell apoptosis [16].

Several previous studies suggested that there is an intrinsic balance between AR and Nur77 in cancer cells. Nur77 mRNA could be dramatically induced by stimulation of synthetic androgen in androgen-responsive LNCaP prostatic cancer cells [17, 18]. In our study on prostate cancer specimen, we noticed that the expressions of AR and Nur77 are positively correlated. More importantly, we found Nur77 over-expression can greatly inhibit ADT-induced metastasis feature of prostate cancer cells which have driven us to perform the further mechanism study on the roles of Nur77 in metastasis of prostate cancer.

Materials and methods

Patients and tissue samples

All tissue samples were obtained from primary tumors during radical surgery at the Nanjing First Hospital from January 11, 2014 to April 2, 2015. Tissues were "snap-frozen" in liquid nitrogen and stored at −70 °C. Regions were manually dissected from the frozen blocks to provide a consistent tumor cell content of more than 70% for analysis. The majority of prostate cancer patients was at the II–III stage of malignancy progression according the TNM staging system. All people who conducted the tissue sample analysis were blind to patient information during and after the experiments until data analysis. Patients were provided written informed consent and the study protocol was approved by the Ethical Committee of Nanjing First Hospital in accordance with the Helsinki Declaration of 1975.

Reagents

Casodex was purchased from Toronto Research Chemicals (Toronto, ON, Canada). MDV3100 was purchased from Selleck Chemicals (Houston, Boston, USA). Fetal bovine serum (FBS), RPMI-1640 medium and transwell culture plates were from GIBCO. Matrigel was from BD Company. TRIzol Reagent was purchased from Invitrogen (Invitrogen, USA). SYBR Green PCR Master Mix was bought from Life Technologies. Transforming Growth Factor-β (TGF-β) and DHT (D-077) were purchased from Sigma-Aldrich. All other chemicals used in this study were at least analytical grade if without specific indication. The antibodies used in this study were summarized in Table 1.

Table 1 The antibodies used in this study

Targeted protein	Source	Company	Application	Dilution ratio
Androgen receptor	Mouse	Abcam	Western blot	1:1000
			ELISA	1:5000
	Rabbit	Abcam	ELISA	1:5000
Nur77	Rabbit	Santa cruz	Western blot	1:1200
			ELISA	1:4000
Nur77	Goat	Sigma-Aldrich	ELISA	1:10,000
Snail	Mouse	Abcam	Western blot	1:1000
E-Cadherin	Rabbit	Abcam	Western blot	1:1500
TGF-β	Rabbit	Abcam	Western blot	1:2000
MMP9	Rabbit	Abcam	Western blot	1:2000
β-actin	Rabbit	CST	Western blot	1:1000
Goat anti-mouse HRP	Goat	CST	Western blot	1:2000
Goat anti-rabbit HRP	Goat	Santa cruz	Western blot	1:3000

ELISA

A double-antibody sandwich method was used to detect the targeted proteins [19, 20]. Briefly, the first primary antibody was appropriately diluted with carbonate buffer and coated on 96-well polystyrene plates at 4 °C overnight. Next, 3% of bovine serum albumin (BSA) was used for blocking. The samples were incubated at room temperature for 1 h. Subsequently, the second primary antibody was added and incubated at room temperature for 1 h. After washing, HRP-conjugated secondary antibody was added and incubated for 1 h. Upon chromogenic termination, the OD490 values were detected using a plate reader.

Cell culture

The VCaP, PC3 and HCI-H660 cell lines were purchased from American Type Culture Collection (ATCC, Rockville, MD, USA). The VCaP cells were cultured in Dulbecco's modified eagle medium (DMEM, Gibco 10313-039) with 4 mM glutamine (Invitrogen), FBS (Omega Scientific) and 10 nM DHT in Corning flasks. PC3 cells were cultured in DMEM that was supplemented with 5% FBS, penicillin and streptomycin. The NCI-H660 cells were cultured in Ham's F12 medium (Gibco) with 10% FBS, 25 ng/ml cholera toxin, 10 ng/ml EGF and 10 nM DHT. For Casodex and MDV treatment, each drug was added into medium up to 10 μM. For DHT treatment, the final concentration of DHT in medium was added up to 100 nM for 2 days before the cells were used in the following assays if without any other specification. For TGF-β treatment, TGF-β was added into medium to 5 ng/ml for 1 day before the cells were used in the following assays.

Nur77 over-expression

The detailed method for plasmid construction and virus production was described in our previous research [7]. Control or Nur77 over-expression virus was applied on the targeted cells for 12 h. After 48 h, the transducted cells were selected with puromycin.

Nur77 knockdown

Short hairpin RNA (shRNA) of Nur77 was synthesized and cloned into pLKO.1 vector. The mature sequences of Nur77 shRNA are: 5′-tccctggcttcattgagctt-3′ and 5′-tgctacaccg-gctgcagtgtgc-3′, respectively. Lentiviral particles were produced and applied on the target cells and drug-selection was performed following the methods described in the previous study [7].

Western blot

Cells were lysed in lysis buffer containing the proteinase inhibitor cocktail (Roche, Nutley, NJ, USA), and protein concentrations were measured with the BCA method (Pierce Chemical, Rockford, IL, USA). 30 μg of proteins were separated via SDS-PAGE, and transferred to Immobilon-P transfer membranes. The membranes were blocked in 3% BSA and incubated overnight at 4 °C with the appropriate primary antibodies. Then, the membranes were incubated with HRP-conjugated secondary antibodies after washing. And the signal was detected with ECL detection reagent (Beyotime, P0018) and captured on films. We repeated each experiment for several times, presented the typical pictures and quantified the results using ImageJ software from NIH.

Cell invasion assay

The cells were treated with vehicle, Casodex (10 μM) or MDV (10 μM) for 2 days before they were used in this assay. Matrigel was dissolved overnight at 4 °C and added to serum-free medium by 1:8 ratio. 100 μL of diluted matrigel was added into the insert of the transwell (Costar Corning, Schiphol-Rijk, the Netherlands), and then was placed in the incubator until fully solidified; for each group, 1.0×10^4 cells in 200 μL of serum-free medium (the drug treatment was maintained at the same concentration) were seeded on solidified gel, and to the lower chamber, 500 μL of regular medium was added. After 36 h, the insert was taken out, and the residual cells in the insert were wiped out by cotton swab. After being washed by PBS once, the cells were fixed and stained by 0.01% crystal violet for 5 min. Transmembrane cells were counted under microscopy for ten fields.

Quantitative reverse transcription polymerase chain reaction (qRT-PCR)

Cells were washed twice with PBS, and then total RNA was extracted using TRIzol Reagent (Invitrogen, USA). Total RNA was purified on columns (NucleoSpin Total RNA Isolation, Qiagen, Germany). The amount of total RNA was determined by optical density at 260 nm and its purity was estimated by 260/280 nm absorption ratio (higher than 1.8) (NanoDrop spectrophotometer, Thermo Scientific, USA).

Reverse transcription was performed using a Revert Aid™ First Strand cDNA Synthesis Kit (MBI-Fermentas, Thermo Scientific, Rockford, IL, USA). The obtained cDNA was subjected to quantitative PCR using SYBR Green PCR Master Mix (Life Technologies) with the specific primers for each interested genes (Table 2). The amplification cycle was: 95 °C for 20 s, 65 °C for 20 s, and 72 °C for 30 s. Amplification was performed for 40 cycles. β-actin was used as

Table 2 The primers used in qRT-PCR

Targeted gene	Sequence
Nur77	
F	5′-TTTCCTTCAGTCCTCCCAC-3′
R	5′-AGAAGTGGGTGCCAAACCT-3′
MMP9	
F	5′-CCACCCTTGTGCTCTTCCCTG-3′
R	5′-TCTGCCACCCGAGTGTAACCA-3′
Snail	
F	5′-AGCGAGCTG CAGGACTCTA-3′
R	5′-TGTCCTCATCTGACAGGGA-3′
β-actin	
F	5′-AGAGCTACGAGCTGCCTGAC-3′
R	5′-AGCACTGTGTTGGCGTACAG-3′

the internal control for calculation. The primers used in this current study are listed in Table 2.

Prediction of promoter regions

The DNA sequences of interested genes were obtained from Ensembl genome database. The proximal promoter regions of Nur77, Snail and MMP9 (Matrix metallopeptidase 9) genes used in the current study were − 850 to + 150 bp, − 301 to + 143 bp and − 597 to + 157 bp, respectively. The promoter sequences were analyzed for binding sites using an online transcription factor prediction software, PROMO [21].

Luciferase assay

The proximal promoter regions were amplified from the genomic DNA of NCI-H660 cells and cloned into pGL3 Luciferase Reporter Vector (Promega Corporation) using NheI and XhoI sites. For activity analysis of different parts of Nur77 promoter, DNA fragments with indicated lengths were amplified using PCR and inserted into pGL3 Luciferase Reporter Vector. The primers for cloning of luciferase reporters are listed in Table 3. The pGL3-derived plasmid (3 μg) was transfected into NCI-H660 cells with pCR3.1 β-galactosidase plasmid (1 μg, as a control of transfection efficiency) using lipofectamine 2000 (Invitrogen). After appropriate treatments, cells were lysed and assayed for luciferase and β-galactosidase activity. The relative luciferase activity was obtained by normalizing luciferase activity against β-gal activity.

Statistics

Quantitative results are shown as the mean ± S.D. Statistical analyses were performed by Student's *t* test or ANOVA. The significances were defined as *, $p \le 0.05$; **, $p \le 0.01$; ***, $p \le 0.001$; #, $p > 0.05$. Pearson correlation analysis was performed using SPSS 16.0 to examine the relationship between AR and Nur77 expressions.

Results

Nur77 expression is positively correlated with AR expression in prostate tumors and cancer cell lines

Since AR is critically important in the development of prostate cancer, we first tested AR expression in tumors and paratumor tissues of prostate cancer patients by ELISA. As shown in Fig. 1a, the expression of AR in tumor tissues was significantly higher than that in paratumor tissues. Since we were interested in the roles of Nur77 in prostate cancer, we also measured Nur77 expression in these tissues and found that the expression of Nur77 in tumor tissues was also significantly higher than that in paratumor tissues (Fig. 1b). In addition, with Pearson correlation analysis, we found that Nur77 expression is positively and significantly associated with AR expression ($p = 0.036$, $r = 0.460$) (Fig. 1c). Also, we tested AR and Nur77 protein expression in three prostate cancer cells, namely PC3, NCI-H660 and VCaP. Data showed that in cell lines with higher AR expression, for example, NCI-H660 and VCaP cell lines, Nur77 was also expressed in higher levels. On the contrary, in PC3 cell line which is AR negative, Nur77 exhibited the lowest expression level (Fig. 1d).

Table 3 The primers for cloning of luciferase reporters

Target gene	Region	Forward	Reverse
Nur77	− 850 to + 150	5′-CTAGCTAGCGTCAGCTGGGTGCGGTGGCTCA-3′	5′-CCCTCGAGAGCCCCACCCCCATCTCCT-3′
	− 700 to + 150	5′-CTAGCTAGCATGCCTGTAAACCCAGCTAC-3′	
	+ 1 to + 150	5′-CTAGCTAGCTTCCTGGTGTAAGCTTTGG-3′	
	+ 101 to + 150	5′-CTAGCTAGCGGTTGGAGGTAGGTAT-3′	
Snail	− 301 to + 143	5′-CTAGCTAGCTCGCTTCGCTCGACGTC-3′	5′-CCCTCGAGCTGGATTAGAGTCCTGCA-3′
MMP9	− 597 to + 157	5′-CTAGCTAGCCCCAGCCTTGCCTAGCAGA-3′	5′-CCCTCGAGCTCTGCCAGCTGCCTGTC-3′

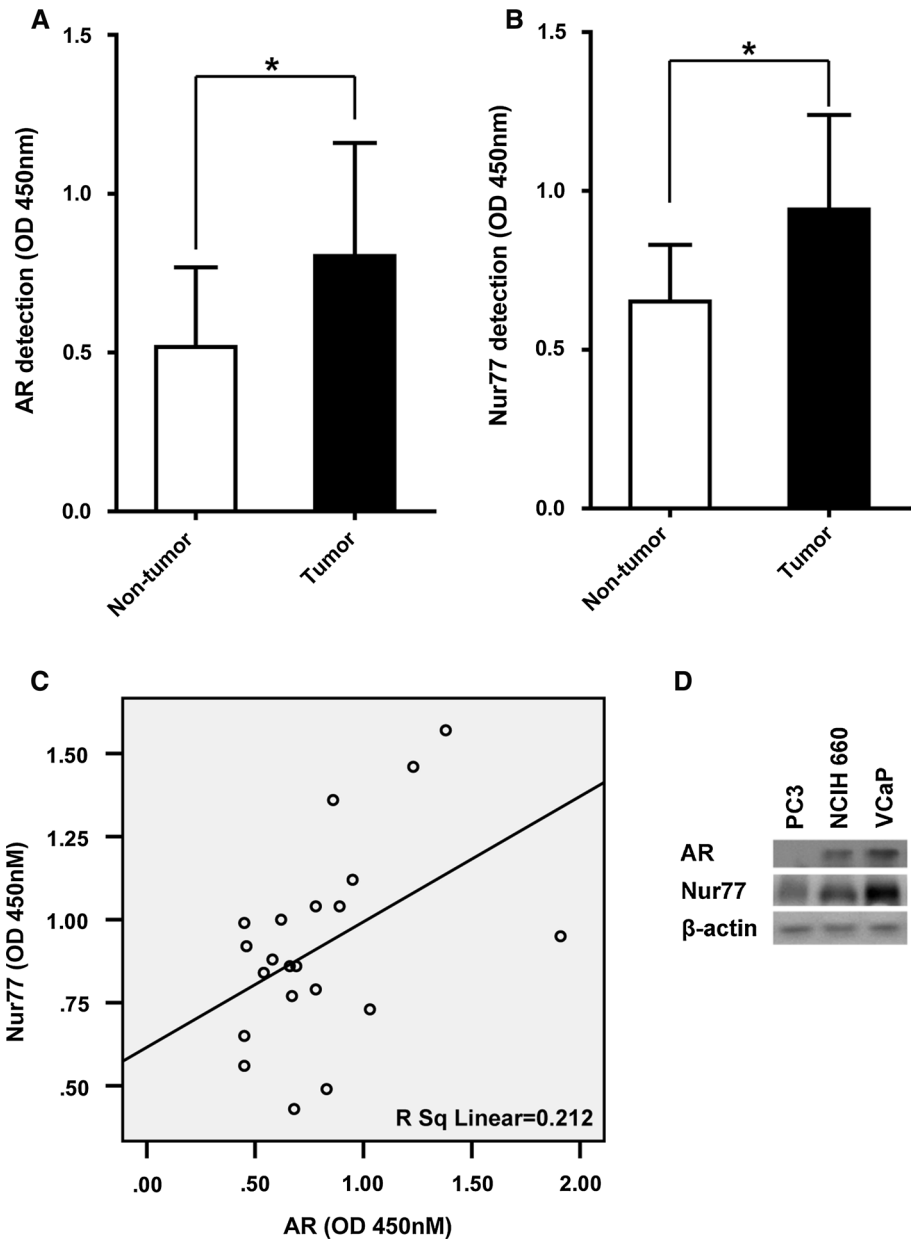

Fig. 1 Expression levels of AR and Nur77 in patients' specimens and cell lines. **a**, **b** Protein levels of AR and Nur77 were detected by ELISA in paratumor tissues and tumor tissues in patients' specimens, respectively. Mean ± SD, $n = 21$. **c** The Pearson correlation analysis of the levels of AR and Nur77. **d** The protein levels of AR and Nur77 in PC3, NCI-H660 and VCaP cells

Nur77 is positively regulated by AR-signaling at transcriptional level in NCI-H660 cells

Given the close correlation between AR and Nur77 expression as shown in Fig. 1, it seems intriguing to identify whether Nur77 is regulated by AR-signaling in prostate cancer cells. Since NCI-H660 cell line has moderate expression levels of AR and Nur77 that may facilitate our study, we selected this cell line as our major study model. We first treated NCI-H660 cells with DHT. The results showed that DHT treatment increased Nur77 expression significantly at both mRNA and protein levels ($p < 0.01$ and $p < 0.05$, respectively) (Fig. 2a–c). On the contrary, when cells were treated with AR antagonist Casodex and MDV, data showed that suppression of AR-signaling significantly inhibited Nur77 expression (Fig. 2d–f). As a next step, we mapped the sequence of Nur77 promoter and identified three AR-binding sites (Fig. 2g). We hypothesized that these AR-binding sites are involved in Nur77 expression regulation. To test this hypothesis, we successfully engineered luciferase reporters with full length Nur77 promoter and several truncated promoters of Nur77 and transfected these plasmids into NCI-H660 cells. The results of luciferase activity assay showed that full length Nur77 promoter (with all three AR-binding sites) exhibited the highest transcription activities, which was followed by the truncated promoter with two AR-binding sites and the truncated promoter with only 1 AR-binding site, respectively, indicating all three

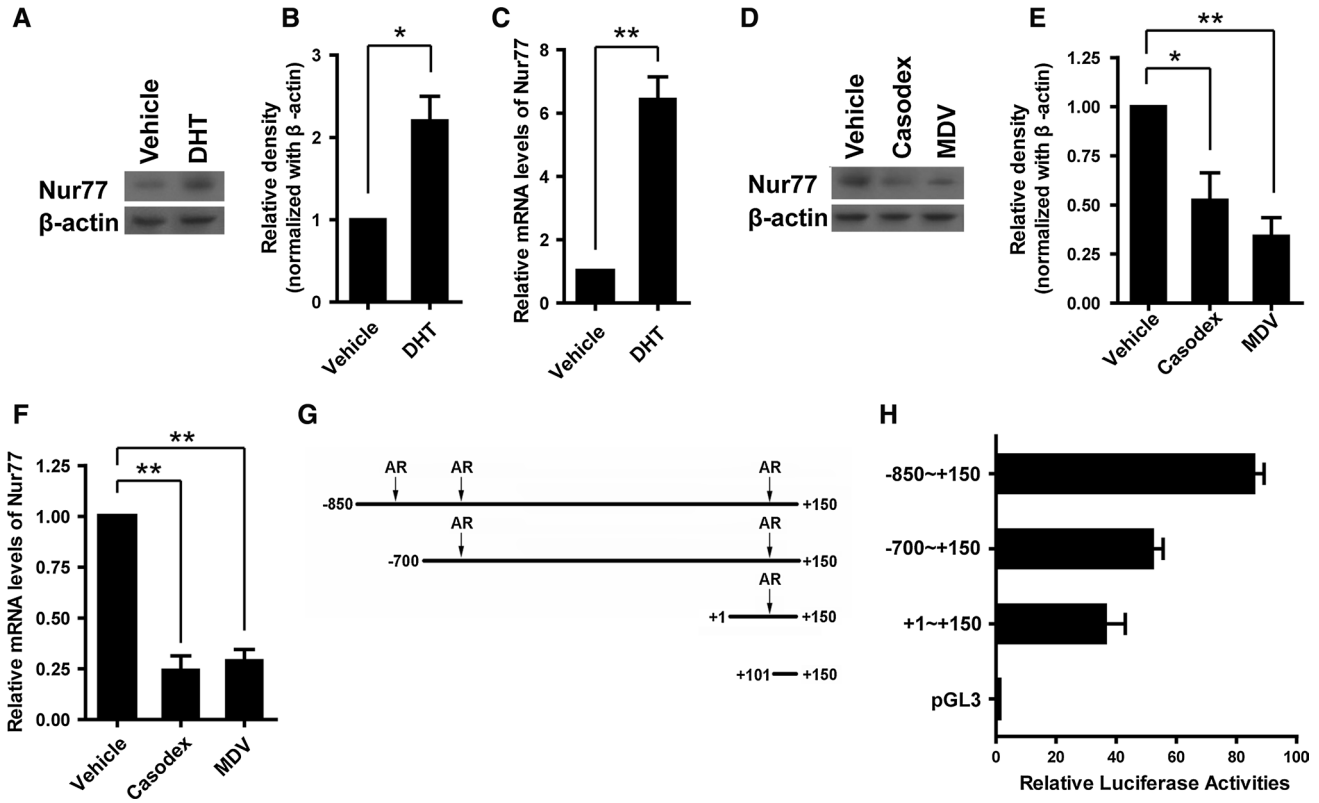

Fig. 2 Nur77 is positively regulated by AR-signaling at transcriptional level in NCI-H660 cells. **a**, **b** The typical picture and quantification results of Nur77 western in NCI-H660 cells with or without DHT treatment. For DHT treatment, the final concentration of DHT in medium was added up to 100 nM for 2 days before the cells were used in the following assays. **c** The relative mRNA levels of Nur77 in NCI-H660 cells with or without DHT treatment. **d**, **e** The typical picture and quantification results of Nur77 western in NCI-H660 cells treated with vehicle, Casodex or MDV3100 (10 μM for 2 days). **f** The mRNA levels of Nur77 in NCI-H660 cells treated with vehicle, Casodex or MDV3100. **g** The scheme of the Nur77 promoters with a series of AR-binding site deletion. The consensus sequence of AR-binding site on proximal promoter region of Nur77 is TGTCC (for −762 to −758, −615 to −611, +89 to +93). **h** The luciferase activities of NCI-H660 cells transfected with different pGL3-derived plasmids, mean ± SD, $n = 3$

AR-binding sites are implicated in AR-mediated Nur77 expression (Fig. 2h). In addition, we tested the luciferase activities of the cells transfected with full length Nur77 promoter and treated with vehicle, Casodex or MDV. The results showed that treatment with Casodex or MDV significantly decreased the luciferase activities of the cells (Fig. S1). All these data demonstrate that Nur77 expression is positively regulated by AR-signaling at transcriptional level in NCI-H660 cells.

Casodex or MDV treatment promoted invasion of prostate cancer cells while inhibited the growth of these cells

In clinic, androgen deprivation is a very important treatment strategy for prostate cancers. However, recent studies have showed that certain anti-androgen treatments increased invasion of prostate cancer cells while inhibited the growth of these cells [5, 6]. Indeed, in our in vitro experiments, AR antagonists Casodex or MDV treatment significantly inhibited prostate cancer cell growth in both NCI-H660 and VCaP cells (Fig. 3a, b). Interestingly, Casodex and MDV treatment changed the epithelial-like morphology (flat and polygonal) of NCI-H660 cells to mesenchymal-like morphology (spindle-like or fibroblast-like morphology) as shown in Fig. 3c. More importantly, Casodex and MDV treatment significantly promoted invasion of both NCI-H660 and VCaP cells measured by transwell assays (Fig. 3d–f). Consistent with these data, we also found up-regulation of TGF-β, MMP9 and Snail protein expression, which were thought to facilitate cancer cell invasion in NCI-H660 cells following Casodex or MDV treatment (Figs. 3g, S2). On the contrary, we were also able to show the down-regulation of E-Cadherin, a suppressor of cell migration following Casodex or MDV treatment (Figs. 3g, S2).

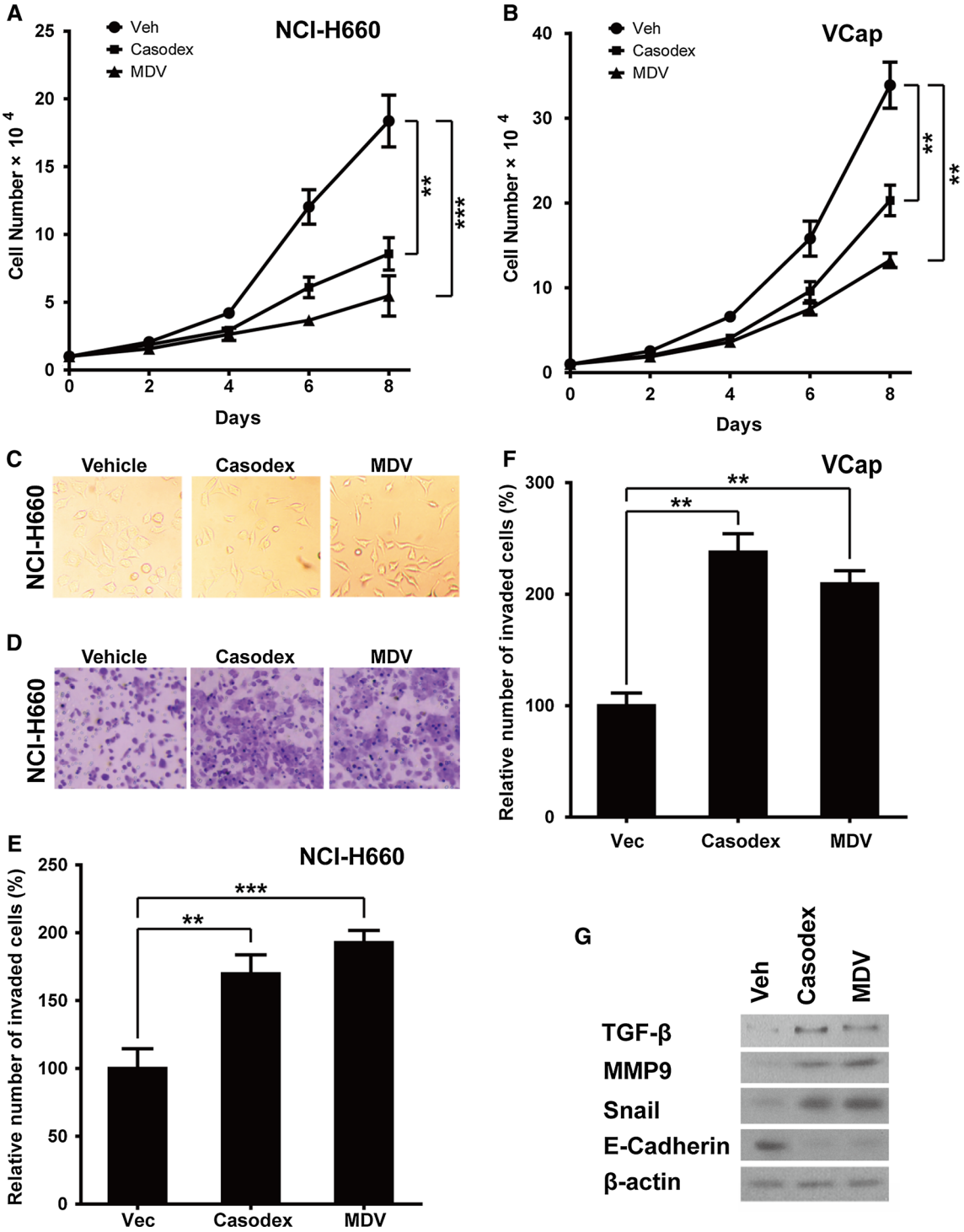

Fig. 3 Cadodex and MDV treatment suppressed the growth of prostate cancer cells, but promoted invasion of prostate cancer cells. **a**, **b** Growth curves of NCI-H660 and VCaP cells treated continuously with vehicle, 10 μM of Casodex or 10 μM of MDV3100, mean ± SD, $n = 3$. **c** The phase contrast micrographs of above cells. **d** Representative pictures of NCI-H660 cells in transwell invasion assay. **e**, **f** Relative numbers of invaded cells of NCI-H660 and VCaP cells with different treatments, mean ± SD, $n = 3$. **g** The protein levels of TGF-β, MMP9, Snail and E-Cadherin in NCI-H660 cells treated with vehicle, Casodex or MDV3100 (10 μM for 2 days), mean ± SD, $n = 3$

Nur77 over-expression inhibited androgen antagonism-mediated NCI-H660 cell invasion

As described by Lin et al., TGF-β1-MMP9 signaling pathway plays a pivotal role in prostate cancer cell migration following Casodex or MDV treatment [5]. Recently, Zerr-Palumbo et al. successfully characterized Nur77 as a potent endogenous inhibitor for TGF-β signaling [22]. In addition, our data showed that Casodex or MDV treatment decreased the expression of Nur77 in NCI-H660 cells. In light of these data, we felt imperative to explore the potential roles of Nur77 in TGF-β-mediated ADT-induced prostate cancer invasion. As the first step, we engineered Nur77 over-expression in NCI-H660 cells and the relative mRNA and protein expression levels of Nur77 were shown in Fig. 4a, b. As expected, Nur77 over-expression resulted in a dramatic inhibition on Casodex or MDV treatment induced cell invasion (Fig. 4c). In addition, we found that while up-regulation of TGF-β after Casodex or MDV treatment remained unchanged, Nur77 over-expression largely abolished up-regulation of MMP9 and Snail expression and the down-regulation of E-Cadherin expression (Fig. 4d). Since MMP9 and Snail are typical downstream target genes of TGF-β, these data strongly suggested that the function of Nur77 may lies on its suppressive roles on the transmission of TGF-β-signaling. In addition, we tested Smad3-signaling which is the classical effector of TGF-β-signaling. The results showed that activation of Smad3-signaling manifested by up-regulation of phosphor-Smad3 was not interrupted by Nur77 over-expression (Fig. 4e). This result suggested the selective

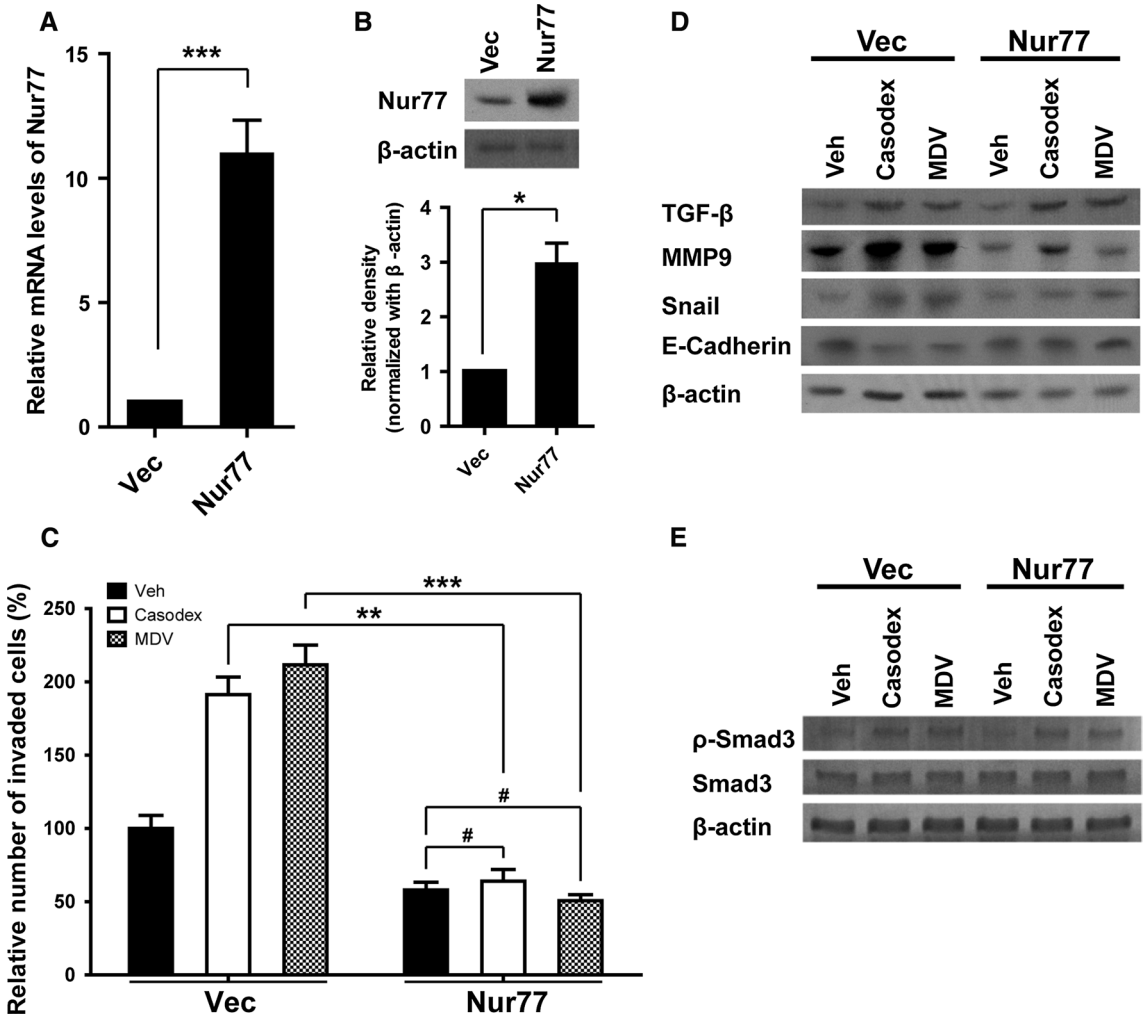

Fig. 4 Nur77 over-expression blocked invasion-promoting effect of ADT. **a** The mRNA level of Nur77 in NCI-H660 cells with or without Nur77 over-expression. **b** The typical picture and quantification results of Nur77 western in NCI-H660 cells with or without Nur77 over-expression. **c** Relative numbers of invaded cells of NCI-H660 cells with or without Nur77 over-expression treated with vehicle, Casodex or MDV3100, mean ± SD, $n = 3$. **d** The protein levels of TGF-β, MMP9, Snail and E-Cadherin in above cells. **e** The protein levels of phosphor-Smad3 and total Smad3 in above cells

nature of the inhibitory effects of Nur77 over-expression on TGF-β-signaling.

Nur77 inhibited TGF-β-induced cell invasion by inhibiting the transcription of TGF-β target genes

To further test our hypothesis, we directly treated NCI-H660 cells with TGF-β protein. Data showed that TGF-β dramatically enhanced cell invasion (Fig. 5a). As expected, Nur77 over-expression greatly abolished TGF-β-induced cell invasion (Fig. 5a). In line with this data, we also observed that Nur77 over-expression abolished TGF-β-induced up-regulation of MMP9 and Snail expression and down-regulation of E-Cadherin (Fig. 5b). In addition, we were able to show that Nur77 over-expression greatly inhibited TGF-β-induced transcription of Snail gene (Fig. 5c). As shown in Fig. 5d, there are four SP1 binding sites which were previously proved to be binding docks for Nur77 [22] in the promoter region of Snail gene. The results of luciferase reporter assay showed that Nur77 over-expression dramatically inhibited TGF-β-mediated transcription of Snail gene (Fig. 5e). In addition, we also confirmed that TGF-β treatment can induce MMP9 transcription and Nur77 over-expression totally abolished this effect of TGF-β in NCI-H660 cells (Fig. S3).

Nur77 knockdown exacerbates TGF-β-induced cell invasion of NCI-H660 cells

To further confirm our hypothesis, as mentioned above, we engineered two shRNAs of Nur77 in NCI-H660 cells (Fig. 6a). As shown in Fig. 6a, b, Nur77 knockdown in NCI-H660 cells with basal conditions increased invasion and protein levels of MMP9 and Snail in these cells. As expected, Nur77 knockdown in this experimental setting decreased E-cadherin expression. In addition, data showed Nur77 knockdown with significantly increased cell invasion following TGF-β exposure (Fig. 6c), which is in line with the augmented expression of MMP9 and Snail protein and the down-regulation of E-Cadherin (Fig. 6d) as well as enhanced Snail mRNA expression (Fig. 6e).

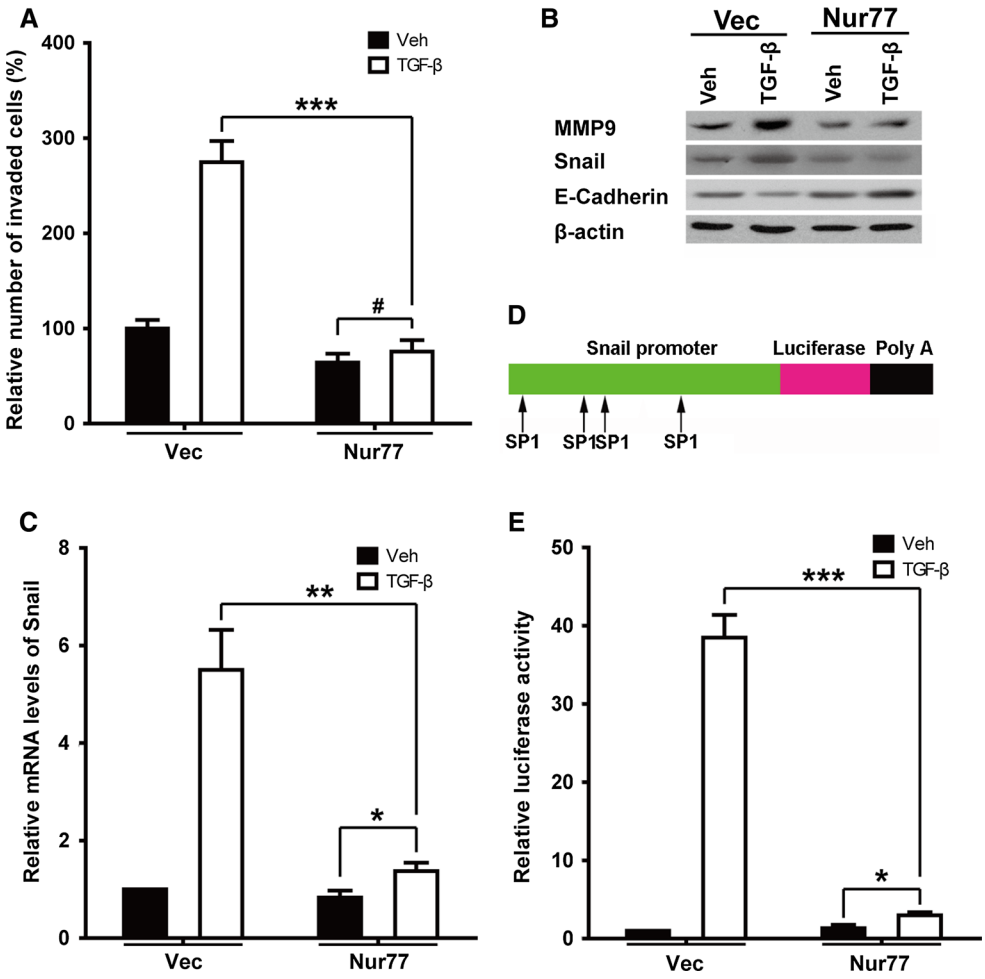

Fig. 5 Nur77 inhibits TGF-β-induced cell invasion by negatively regulating the promoter activities of TGF-β target genes. **a** The relative numbers of invaded cells of NCI-H660 cells with or without Nur77 over-expression treated with vehicle or TGF-β, mean ± SD, $n = 3$. **b** The protein levels of MMP9, Snail and E-Cadherin in above cells. **c** The mRNA levels of Snail in above cells, mean ± SD, $n = 3$. **d** The scheme of Snail promoter showing four SP1 binding sites. **e** The luciferase activities of above cells transfected with pGL3-derived plasmid containing Snail promoter, mean ± SD, $n = 3$

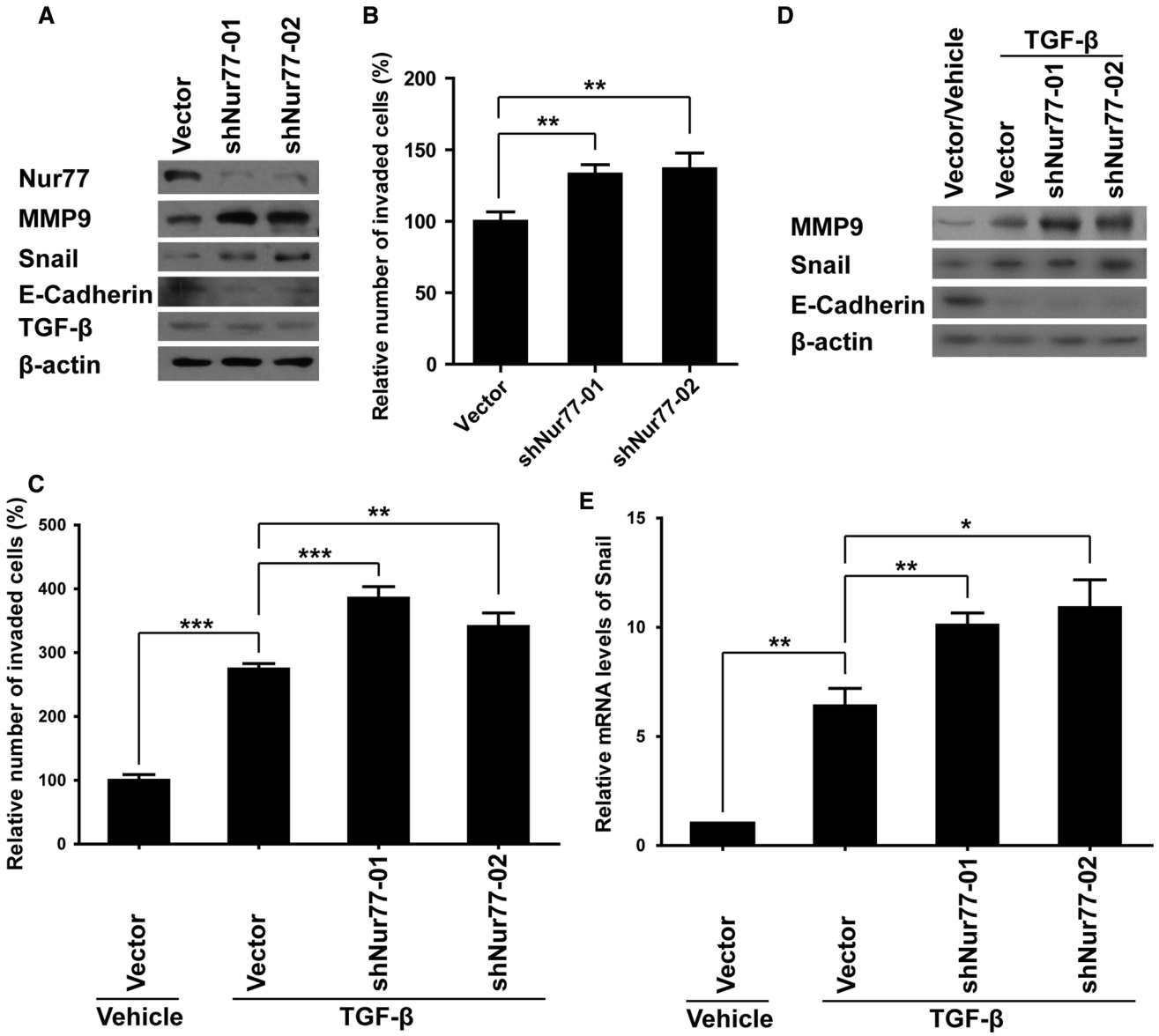

Fig. 6 Nur77 knockdown exaggerates TGF-β-induced cell invasion. **a** The protein levels of Nur77, MMP9, Snail, E-Cadherin and TGF-β in NCI-H660 cells with or without Nur77 knockdown. **b** The relative numbers of invaded cells of NCI-H660 cells with or without Nur77 knockdown. **c** The relative numbers of invaded cells with or without Nur77 knockdown treated with vehicle or TGF-β (5 ng/ml for 1 day), mean ± SD, $n = 3$. **d** The protein levels of TGF-β, MMP9, Snail and E-Cadherin in **c**. **e** The mRNA levels of Snail of above cells, mean ± SD, $n = 3$

Discussion

Currently, ADT remains to be the mainstay of the management of locally advanced, metastatic and recurrent prostate cancer patients following the localized treatment [23]. ADT has been well documented for its inhibitory role of prostate cancer progression which is manifested by the dramatic decline of prostate specific antigen (PSA) in approximately 90% of patients [24]. However, after a mean time of 2 or 3 years, most diseases will progress to castration-resistant prostate cancer which is often metastatic with a mean survival between 16 and 18 months [25]. More importantly, several previous studies suggest that metastasis of certain types of prostate cancer may result directly from ADT [26, 27].

TGF-β is a well-documented cytokine which governs tissue fibrosis, growth arrest and cancer cell invasion [28]. In diverse scenarios, TGF-β ligand binds to TGF-β type II serine/threonine kinase receptor, which in turn drives the trans-phosphorylation and activation of TGF-β type I receptor and downstream Smad proteins, which ultimately results in the altered gene expression regulation in the nucleus [28].

Recently, TGF-β was reported to be implicated in prostate cancer cell invasion following androgen antagonism. Lin et al. revealed that abnormal activation of TGF-β/Smad3/MMP9 signaling following Casodex/MDV3100 exposure may account for the enhanced prostate cancer cell invasion [5], which, together with the fact that endogenous Nur77 inhibits TGF-β signaling in a separate study [22], prompt us to hypothesize that Nur77 may exert potent inhibitory role on TGF-β-mediated prostate cancer cell invasion. These data suggested that Nur77 may form a repressive complex to inhibit the transcription of TGF-β target genes by binding with SP1 sites on their promoters. In the currently study, we found that Nur77 over-expression blocks invasion-promoting effect of ADT. The mechanism study showed that Nur77 over-expression greatly inhibits TGF-β-mediated transcription of target genes such as MMP9 and Snail, and the nature of this inhibitory effects of Nur77 on TGF-β-signaling is selective. Smad3-signaling, which is the classical effector of TGF- β pathway, was not interrupted by Nur77 over-expression.

TGF-β activates MMP9 transcription through phosphorylation of Smad3 and the latter activates MMP9 transcription by binding to the Smad response element on MMP9 promoter [29]. Katrin et al. reported that Nur77 inhibits TGF-β-signaling by recruiting a repressor complex on promoter of MMP9 [22]. In light of these findings, we showed that Nur77 over-expression greatly inhibits TGF-β induced MMP9 transcription probably due to the repressive function of Nur77 on MMP9 promoter. Of note, there are also contrary reports of the functions of Nur77 on TGF-β signaling. For example, Zhou et al. reported that Nur77 promotes breast cancer invasion and metastasis by activating TGF-β signaling [30]. We noticed that Nur77 is a transcription factor with versatile natures in different cancers, and it seems that Nur77 action is highly tissue-specific.

Our data also showed that Snail may also be implicated in Nur77-modulated TGF-β signaling which governs prostate cancer cell invasion following androgen antagonism. Peinado H et al. showed that TGF-β induces epithelial mesenchymal transition by up-regulating Snail protein [31]. Snail exerts transcriptional inhibitory effects via binding to E-box motif of target gene promoters [32], such as E-Cadherin which is essential for cell adhesion. Loss of E-Cadherin facilitates cell migration [33, 34]. Consistent with these observations, our data suggested that Snail is highly inducible following TGF-β treatment and Nur77 over-expression inhibits TGF-β-induced Snail transcription which in turns represses the expression of E-Cadherin.

In short, metastasis of prostate cancer following ADT remains to be a major obstacle for optimal outcome of prostate cancer management. TGF-β up-regulation and the subsequent transcription of TGF-β target genes following ADT drives prostate cancer cell invasion. Given the specific inhibitory role of Nur77 on transcription of certain TGF-β target genes, Snail and MMP9, ADT-mediated Nur77 down-regulation facilitates transcription of TGF-β target genes, and therefore potentiates TGF-β function (Fig. S4). Our data highlights that Nur77 over-expression can exert anti-metastatic effects on prostate cancer cells via a mechanism involving inhibition of transcription of TGF-β target genes such as Snail and MMP9, which contributes a promising,complementary therapeutic strategy on top of classic ADT therapy and warrants further investigation.

Acknowledgements We thank the team of Urology Department of Nanjing First Hospital for the technical support in the whole research project.

Author contributions WJ and SX designed the study, performed the experiments and drafted the manuscript. SX and SH revised the study protocol, supervised the whole project and revised the final draft. YX verified the analytical methods and made the revised draft.

Funding This work was funded by Nanjing Medical Science and Technology Development Program (Serial No. ykk15904 to WJ).

Compliance with ethical standards

Conflict of interest All authors agreed that there is nothing to disclose for the current study.

Ethical approval The study protocol was approved by the Ethical Committee of Nanjing First Hospital in accordance with the Helsinki Declaration of 1975.

Informed consent Patients were provided written informed consent prior to be enrolled into the study.

References

1. Siegel R, Naishadham D, Jemal A. Cancer statistics, 2012. CA Cancer J Clin. 2012;62(1):10–29. https://doi.org/10.3322/caac.20138.
2. Mohler JL, Kantoff PW, Armstrong AJ, Bahnson RR, Cohen M, D'Amico AV, et al. Prostate cancer, version 1.2014. J Natl Compr Cancer Netw : JNCCN. 2013;11(12):1471–9.
3. Perlmutter MA, Lepor H. Androgen deprivation therapy in the treatment of advanced prostate cancer. Rev Urol. 2007;9(Suppl 1):S3–8.
4. Nouri M, Ratther E, Stylianou N, Nelson CC, Hollier BG, Williams ED. Androgen-targeted therapy-induced epithelial mesenchymal plasticity and neuroendocrine transdifferentiation in prostate cancer: an opportunity for intervention. Front Oncol. 2014;4:370. https://doi.org/10.3389/fonc.2014.00370.
5. Lin TH, Lee SO, Niu Y, Xu D, Liang L, Li L, et al. Differential androgen deprivation therapies with anti-androgens casodex/bicalutamide or MDV3100/Enzalutamide versus anti-androgen receptor ASC-J9(R) Lead to promotion versus suppression of prostate cancer metastasis. J Biol Chem. 2013;288(27):19359–69. https://doi.org/10.1074/jbc.M113.477216.
6. Xie H, Li L, Zhu G, Dang Q, Ma Z, He D, et al. Infiltrated pre-adipocytes increase prostate cancer metastasis via modulation of the

miR-301a/androgen receptor (AR)/TGF-beta1/Smad/MMP9 signals. Oncotarget. 2015;6(14):12326–39. https://doi.org/10.18632/oncotarget.3619.
7. Wu J, Liu J, Jia R, Song H. Nur77 inhibits androgen-induced bladder cancer growth. Cancer Invest. 2013;31(10):654–60. https://doi.org/10.3109/07357907.2013.853077.
8. Maruyama K, Tsukada T, Ohkura N, Bandoh S, Hosono T, Yamaguchi K. The NGFI-B subfamily of the nuclear receptor superfamily (review). Int J Oncol. 1998;12(6):1237–43.
9. Mohan HM, Aherne CM, Rogers AC, Baird AW, Winter DC, Murphy EP. Molecular pathways: the role of NR4A orphan nuclear receptors in cancer. Clin Cancer Res Off J Am Assoc Cancer Res. 2012;18(12):3223–8. https://doi.org/10.1158/1078-0432.CCR-11-2953.
10. Ranhotra HS. The NR4A orphan nuclear receptors: mediators in metabolism and diseases. J Recept Signal Transduct Res. 2015;35(2):184–8. https://doi.org/10.3109/10799893.2014.948555.
11. Kolluri SK, Zhu X, Zhou X, Lin B, Chen Y, Sun K, et al. A short Nur77-derived peptide converts Bcl-2 from a protector to a killer. Cancer Cell. 2008;14(4):285–98. https://doi.org/10.1016/j.ccr.2008.09.002.
12. Wilson AJ, Arango D, Mariadason JM, Heerdt BG, Augenlicht LH. TR3/Nur77 in colon cancer cell apoptosis. Can Res. 2003;63(17):5401–7.
13. Wu Q, Liu S, Ye XF, Huang ZW, Su WJ. Dual roles of Nur77 in selective regulation of apoptosis and cell cycle by TPA and ATRA in gastric cancer cells. Carcinogenesis. 2002;23(10):1583–92.
14. Xie L, Jiang F, Zhang X, Alitongbieke G, Shi X, Meng M, et al. Honokiol sensitizes breast cancer cells to TNF-alpha induction of apoptosis by inhibiting Nur77 expression. Br J Pharmacol. 2016;173(2):344–56. https://doi.org/10.1111/bph.13375.
15. Lee KW, Cobb LJ, Paharkova-Vatchkova V, Liu B, Milbrandt J, Cohen P. Contribution of the orphan nuclear receptor Nur77 to the apoptotic action of IGFBP-3. Carcinogenesis. 2007;28(8):1653–8. https://doi.org/10.1093/carcin/bgm088.
16. Agostini-Dreyer A, Jetzt AE, Stires H, Cohick WS. Endogenous IGFBP-3 mediates intrinsic apoptosis through modulation of Nur77 phosphorylation and nuclear export. Endocrinology. 2015;156(11):4141–51. https://doi.org/10.1210/en.2015-1215.
17. Uemura H, Chang C. Antisense TR3 orphan receptor can increase prostate cancer cell viability with etoposide treatment. Endocrinology. 1998;139(5):2329–34. https://doi.org/10.1210/endo.139.5.5969.
18. Hu YL, Zhong D, Pang F, Ning QY, Zhang YY, Li G, et al. HNF1b is involved in prostate cancer risk via modulating androgenic hormone effects and coordination with other genes. Genet Mol Res GMR. 2013;12(2):1327–35. https://doi.org/10.4238/2013.April.25.4.
19. Feng X, Ma JW, Sun SQ, Guo HC, Yang YM, Jin Y, et al. Quantitative detection of the foot-and-mouth disease virus serotype O 146S antigen for vaccine production using a double-antibody sandwich ELISA and nonlinear standard curves. PLoS One. 2016;11(3):e0149569. https://doi.org/10.1371/journal.pone.0149569.
20. Chen SL, Li YL, Tang Y, Chen ZC, Zhou J, Zhou J, et al. Development and evaluation of a double antibody sandwich ELISA for the detection of human sDC-SIGN. J Immunol Methods. 2016;436:16–21. https://doi.org/10.1016/j.jim.2016.05.011.
21. Wei CL, Lin YC, Chen TA, Lin RY, Liu TH. Respiration detection chip with integrated temperature-insensitive MEMS sensors and CMOS signal processing circuits. IEEE Trans Biomed Circuits Syst. 2015;9(1):105–12. https://doi.org/10.1109/TBCAS.2014.2315532.
22. Palumbo-Zerr K, Zerr P, Distler A, Fliehr J, Mancuso R, Huang J, et al. Orphan nuclear receptor NR4A1 regulates transforming growth factor-beta signaling and fibrosis. Nat Med. 2015;21(2):150–8. https://doi.org/10.1038/nm.3777.
23. Huggins C. Prostatic cancer treated by orchiectomy; the 5 year results. J Am Med Assoc. 1946;131:576–81.
24. Harris WP, Mostaghel EA, Nelson PS, Montgomery B. Androgen deprivation therapy: progress in understanding mechanisms of resistance and optimizing androgen depletion. Nat Clin Pract Urol. 2009;6(2):76–85. https://doi.org/10.1038/ncpuro1296.
25. Marques RB, Dits NF, Erkens-Schulze S, van Weerden WM, Jenster G. Bypass mechanisms of the androgen receptor pathway in therapy-resistant prostate cancer cell models. PLoS One. 2010;5(10):e13500. https://doi.org/10.1371/journal.pone.0013500.
26. Niu Y, Chang TM, Yeh S, Ma WL, Wang YZ, Chang C. Differential androgen receptor signals in different cells explain why androgen-deprivation therapy of prostate cancer fails. Oncogene. 2010;29(25):3593–604. https://doi.org/10.1038/onc.2010.121.
27. Niu Y, Altuwaijri S, Lai KP, Wu CT, Ricke WA, Messing EM, et al. Androgen receptor is a tumor suppressor and proliferator in prostate cancer. Proc Natl Acad Sci USA. 2008;105(34):12182–7. https://doi.org/10.1073/pnas.0804700105.
28. Son H, Moon A. Epithelial-mesenchymal transition and cell invasion. Toxicological Res. 2010;26(4):245–52. https://doi.org/10.5487/TR.2010.26.4.245.
29. Chou YT, Wang H, Chen Y, Danielpour D, Yang YC. Cited2 modulates TGF-beta-mediated upregulation of MMP9. Oncogene. 2006;25(40):5547–60. https://doi.org/10.1038/sj.onc.1209552.
30. Zhou F, Drabsch Y, Dekker TJ, de Vinuesa AG, Li Y, Hawinkels LJ, et al. Nuclear receptor NR4A1 promotes breast cancer invasion and metastasis by activating TGF-beta signalling. Nat Commun. 2014;5:3388. https://doi.org/10.1038/ncomms4388.
31. Peinado H, Olmeda D, Cano A. Snail, Zeb and bHLH factors in tumour progression: an alliance against the epithelial phenotype? Nat Rev Cancer. 2007;7(6):415–28. https://doi.org/10.1038/nrc2131.
32. Nieto MA. The snail superfamily of zinc-finger transcription factors. Nat Rev Mol Cell Biol. 2002;3(3):155–66. https://doi.org/10.1038/nrm757.
33. Batlle E, Sancho E, Franci C, Dominguez D, Monfar M, Baulida J, et al. The transcription factor snail is a repressor of E-cadherin gene expression in epithelial tumour cells. Nat Cell Biol. 2000;2(2):84–9. https://doi.org/10.1038/35000034.
34. Qu SS, Huang Y, Zhang ZJ, Chen JQ, Lin RY, Wang CQ, et al. A 6 week randomized controlled trial with 4 week follow-up of acupuncture combined with paroxetine in patients with major depressive disorder. J Psychiatr Res. 2013;47(6):726–32. https://doi.org/10.1016/j.jpsychires.2013.02.004.